Supplementary Appendix for

An Integrated Circuit for Simultaneous Extracellular Electrophysiology Recording and Optogenetic Neural Manipulation

Chang Hao Chen[1,2], Elizabeth A McCullagh[3], Sio Hang Pun[1], Peng Un Mak[2], Mang I Vai[1,2], Pui In Mak[1,2] , Achim Klug[3], Tim C. Lei[1,4*]

[1] State Key Laboratory of Analog and Mixed-Signal VLSI, University of Macau, Macau, China

[2] Department of Electrical and Computer Engineering, Faculty of Science and Technology, University of Macau, Macau, China

[3] Department of Physiology and Biophysics, University of Colorado School of Medicine, Aurora, Colorado, United States of America

[4] Department of Electrical Engineering, University of Colorado Denver, Colorado, United States of America

*Corresponding author: Tim C. Lei, Department of Electrical Engineering, University of Colorado Denver, Colorado, United States of America (tim.lei@ucdenver.edu; Telephone: +1-303-556-4924)

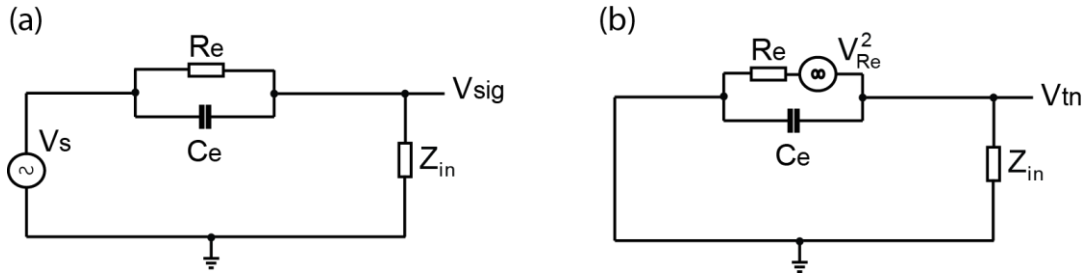

Fig. S1: (a) Circuit to calculate the signal voltage V_{sig} received by the amplifier; (b) Circuit to calculate the thermal noise voltage V_{tn} generated from the metal electrode received by the amplifier.

I. Derivation of the signal-to-noise (SNR) equation

To simplify the derivation, several noise sources in the noise model can be neglected if noise elimination strategies were used. The surrounding neuron background noise V_{nt}^2 can be neglected using a small tip opening (high impedance) metal electrode. The optogenetic photoelectric artifact V_{op}^2 only occurs on the onsets of the optical illumination and can be removed using post-processing signal processing techniques. The power-line interface V_p^2 and the current fluctuation noise V_{EL}^2 can also be eliminated if good grounding strategy around the experimental setup and IC design guidelines were used. In addition, the DC half-cell potential E_j were filtered through the high pass filter preceding the amplifier, and the metal electrode insulating capacitance C_w can also be neglected if good insulating material around the metal electrode were used. Therefore, the signal voltage V_{sig} received by the amplifier frontend can be approximated according to the equivalent circuit depicted in Fig. S1 (a),

$$V_{sig} = V_s \cdot \frac{Z_{in}}{R_e // Z_{Ce} + Z_{in}}$$

Because of the high impedance of the metal electrode, the thermal noise generated by this high impedance dominates the measurable noise of the entire system, the thermal noise voltage V_{tn} received at the amplifier frontend can also be estimated from Fig. S1 (b),

$$V_{tn} = V_{Re} \cdot \frac{Z_{Ce} // Z_{in}}{Z_{Ce} // Z_{in} + R_e}$$

Therefore, the SNR of the amplifier can then be approximated as

$$SNR = \frac{|V_{sig}|}{\sqrt{V_{tn}^2 + V_A^2}} \approx \frac{V_s \left| \frac{Z_{in}}{R_e // Z_{Ce} + Z_{in}} \right|}{\sqrt{V_{Re}^2 \left| \frac{Z_{Ce} // Z_{in}}{Z_{Ce} // Z_{in} + R_e} \right|^2 + V_A^2}}$$

The above equation can be simplified using the assumption that for metal electrode, the impedances of the metal-electrolyte interface leakage resistance Z_{Re} and the electric double layer capacitance C_e are generated experimentally measured to have similar values [1], i.e. $|Z_{Re}| \approx |Z_{ce}|$ or $2\pi R_e C_e \approx 1$.

Since

$$R_e // Z_{Ce} = \frac{R_e}{1 + j2\pi f C_e R_e} \approx \frac{R_e}{1 + j}$$

Therefore,

$$\begin{aligned} \left| \frac{Z_{in}}{R_e // Z_{Ce} + Z_{in}} \right| &\approx \left| \frac{\frac{1}{j2\pi f C_{in}}}{\frac{R_e}{1+j} + \frac{1}{j2\pi f C_{in}}} \right| \\ &\approx \left| \frac{1}{\left(1 + \frac{C_{in}}{2C_e}\right) + j\frac{C_{in}}{2C_e}} \right| \\ &= \frac{1}{\sqrt{\left(1 + \frac{C_{in}}{2C_e}\right)^2 + \left(\frac{C_{in}}{2C_e}\right)^2}} \end{aligned}$$

Also,

$$\begin{aligned} \left| \frac{Z_{Ce} // Z_{in}}{Z_{Ce} // Z_{in} + R_e} \right| &= \left| \frac{1}{1 + j2\pi f R_e (C_{in} + C_e)} \right| \\ &\approx \left| \frac{1}{1 + j(1 + \frac{C_{in}}{C_e})} \right| \\ &= \frac{1}{\sqrt{1 + (1 + \frac{C_{in}}{C_e})^2}} \end{aligned}$$

The SNR of the amplifier can be approximated that

$$SNR \approx \frac{\frac{V_s}{\sqrt{\left(1+\frac{C_{in}}{2C_e}\right)^2+\left(\frac{C_{in}}{2C_e}\right)^2}}}{\sqrt{\frac{V_{Re}^2}{1+(1+\frac{C_{in}}{C_e})^2}+V_a^2}} = \frac{V_s}{\sqrt{\frac{V_{Re}^2}{2}+V_A^2\left[\left(1+\frac{C_{in}}{2C_e}\right)^2+\left(\frac{C_{in}}{2C_e}\right)^2\right]}}$$

II. Thermal characterization of the IC

Temperature increase of the IC was measured before and after a 20 minutes section of laser illumination. The two PMOS arrays were running on their maximum currents of 330 mA with a duty cycle of 3 seconds on and 7 seconds off over the entire 20 minutes period. The duty cycle is chosen to simulate a typical experimental condition of optogenetic neural inhibition to avoid laser toxicity to the neurons. The measurement was performed using a fine-gauge thermal couple (7001H, Physitemp,Instruments, Clifton, NY) over 25 different locations uniformly distributed on the top surface of the IC. The IC temperature before the measurement was 22.4 °C and increased by 3.2 °C to 25.6±0.3 °C in average. The maximum and minimum temperatures were 27.4 and 24.1 °C over the 25 different locations.

III. Power consumption of the IC

Power consumption of the IC was measured under various operational conditions and is tabulated in Table S1. The power consumption of the neural amplifier was 318 μW and the quiescent power consumption of the laser/LED PMOS current driver was 2.23 mW. When the laser/LED PMOS current driver was delivering its maximum current of 330 mA, the power consumption of the entire IC was 1.07 W.

	Neural Amplifier	Laser/LED PMOS Driver	Total Power Consumption
Laser ON (330 mA)	318 µW	1.07 W	1.07 W
Laser Off	318 µW	2.23 mW	2.55 mW

Table S1. Power consumption of the IC under different operational conditions.

IV. Characterization of the illumination noise

The illumination noise was carefully characterized by dipping a metal electrode into a saline solution as a brain phantom and the voltage output of the neural amplifier were measured when the laser was turned on and off at the maximum driving current of 330 mA. The plotted results were shown in Fig. S1. Two abrupt changes - one appeared when the laser was turned on and another one appeared when the laser was off - were observed at the output of the neural amplifier. The voltage swings of the two noises were measured to be 1.16±0.03 mV and 0.65±0.02 mV and the two noises lasted for 4.63±0.38 ms and 4.21±0.96 ms, respectively (n=10).

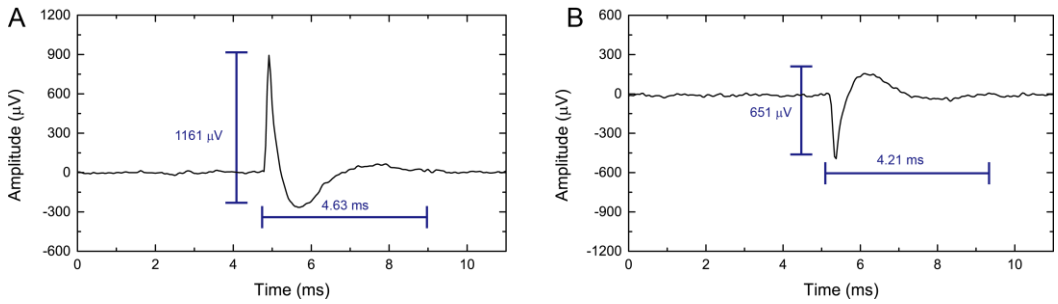

Fig. S1. (A) The illumination noise observed at the output of the neural amplifier when the laser was turned on and (B) when the laser was turned off.

V. Comparison to other amplifier designs

The performance of our neural amplifier was compared to that of a commercial neural amplifier (Isolated bio-amplifier with active probe, ISO-80; World precision instrument, Sarasota, FL). In this measurement, the inputs of the two amplifiers were connected in parallel to a metal electrode to measure the neural response of an anesthetized gerbil in tandem. Other than this difference, the rest of the experimental procedure was identical to Section VI(B) of the main text. Note that under this configuration, the input impedances of both amplifiers are the same due to the parallel connection. As indicative by the measurement result, our neural amplifier has a SNR of 9.14. The ISO-80 amplifier, however, has a higher noise level, which results in a lower SNR of 6.40.

In addition, input impedance of our neural amplifier was compared to those of two other IC neural amplifiers (RHD2000 and RHA2000, Intan, Los Angeles,

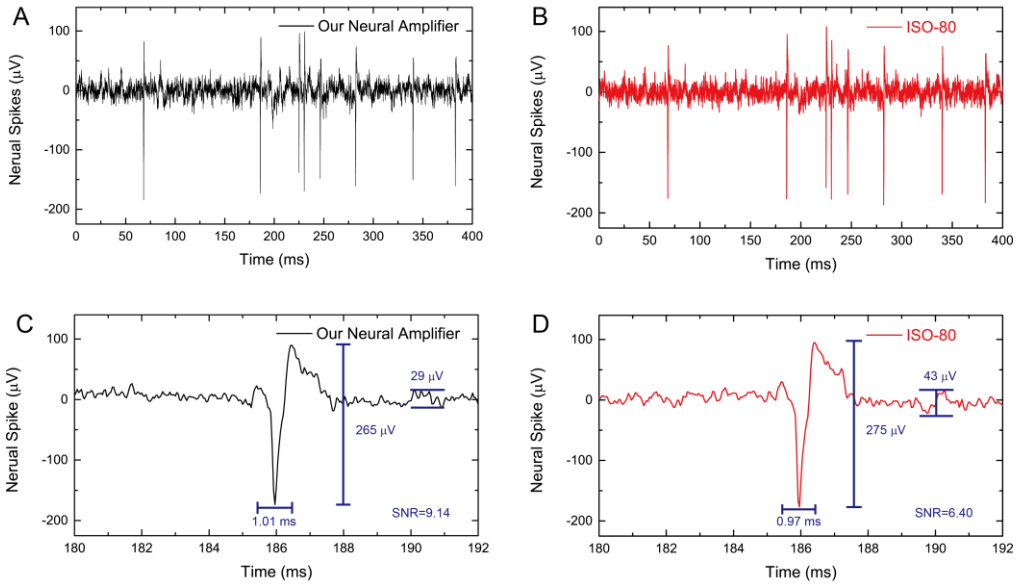

Fig. S2. Comparison of our neural amplifier to ISO-80 amplifier. Neural spikes recorded using our neural amplifier (A) and the ISO-80 amplifier (B). Zoom-in views of one neural spike of our neural amplifier (C) and the ISO-80 amplifier (D).

	Intan RHD2000 Series	Intan RHA2000 Series	Our neural amplifier
Input Impedance (f=10Hz)	1300 MΩ	1300 MΩ	1640 MΩ
Input Impedance (f=1kHz)	13 MΩ	13 MΩ	16.4 MΩ

Table S2. Comparison of the input impedance between two other IC neural amplifiers and our neural amplifier at 10 Hz and 1 KHz.

CA) at both 10 Hz and 1 kHz frequencies and the data was tabulated in Table S1. For both frequencies, our amplifier has higher input impedances, probably due to the use of a dedicated unit-gain stage at the amplifier input to increase the input impedance.

Bibliography

[1] D. R. Humphrey and E. M. Schmidt, “Extracellular Single-Unit Recording Methods,” in *Neurophysiological Techniques*, vol. 15, A. A. Boulton, G. B. Baker, and C. H. Vanderwolf, Eds. 1990, pp. 1–64.